



OPEN Selected microwave irradiation effectively inactivates airborne avian influenza A(H5N1) virus

Pietro Bia¹✉, Margherita Losardo¹, Antonio Manna¹, Silvio Brusaferrero^{2,5}, Gaetano P. Privitera^{3,5} & Alberto Sangiovanni Vincentelli⁴

The highly pathogenic avian influenza A(H5N1) virus threatens animal and human health globally. Innovative strategies are crucial for mitigating risks associated with airborne transmission and preventing outbreaks. In this study, we sought to investigate the efficacy of microwave inactivation against aerosolized A(H5N1) virus by identifying the optimal frequency band for a 10-min exposure and evaluating the impact of varying exposure times on virus inactivation. A(H5N1) was aerosolized and exposed to various microwave frequencies ranging from 8 to 16 GHz for a duration of 10 min. Viral titers were quantified using TCID₅₀, and inactivation was assessed by comparing irradiated samples to controls. The 11–13 GHz band yielded the highest inactivation, with an average 89% mean reduction in A(H5N1) titer, particularly within the 11–12 GHz range, which exhibited peak efficacy. Based on the overall results, the optimal frequency band (8–12 GHz) was further tested with exposure durations of 1, 3, and 5 min. Inactivation was time-dependent, with a 5-minute exposure resulting in a 94% mean reduction, compared to 58% and 48% for 3- and 1-minute exposures, respectively. We conclude that optimized microwave emitters in high-risk environments like poultry farms and veterinary clinics could offer a novel, non-chemical approach to mitigating avian influenza spread and outbreaks.

Keywords Avian influenza, A(H5N1) virus, Radiated microwaves, Frequency bands, Exposure time

The highly pathogenic avian influenza A(H5N1) virus, a member of the *Influenzavirus A* genus within the *Orthomyxoviridae* family, poses a significant global threat to both animal and human health^{1,2}. Since the identification of a particular viral lineage in domestic geese in Guangdong, China, in 1996, this pathogen has led to severe epizootics in poultry populations throughout Asia, Europe, Africa, and North America³. Of particular concern is the virus's ability to cross the species barrier and infect humans, with sporadic cases documented in multiple countries following direct contact with infected animals^{4–6}. Notably, the A(H5N1) virus exhibits a case fatality rate of approximately 50% in affected individuals⁷. Although limited human-to-human transmission has been observed in a small number of family clusters⁸, sustained community spread has not yet been reported. Additionally, this virus has been detected in cattle and their milk, posing a significant risk of transmission to humans^{9,10}. The potential for A(H5N1) to evolve more efficient human-to-human transmission and trigger a global pandemic remains a serious concern for public health authorities worldwide^{5,6}. Furthermore, the possibility of genetic reassortment among avian, swine, and human influenza viruses increases the risk of novel strains emerging with enhanced transmissibility¹¹. Exposure to infected poultry or contaminated environments is the primary risk factor for human infections, placing poultry workers, veterinarians, and healthcare workers at increased risk^{12,13}. In human infections, A(H5N1) targets the alveoli of the lower respiratory tract¹⁴, causing severe viral pneumonia accompanied by a profound dysregulation of the host cytokine response¹⁵. In general, the clinical course is progressive, frequently resulting in acute respiratory distress syndrome and multi-organ failure¹⁶. Consequently, an A(H5N1) outbreak could severely strain healthcare systems^{1,5,6}, highlighting the urgent need for measures to control infections in poultry and cattle to reduce the risk of human exposure.

Electromagnetic radiation within the microwave spectrum, spanning frequencies from 300 MHz to 300 GHz, exhibits non-ionizing properties while possessing sufficient energy to induce molecular vibrations in matter^{17,18}. Among the diverse applications of this vibrational excitation, the phenomenon of resonant energy transfer from microwave radiation to specific acoustic vibrational modes of viral particles has emerged

¹Elettronica S.p.A, Via Tiburtina Valeria, Km 13.700, Rome 00131, Italy. ²Department of Medicine, University of Udine, Udine, Italy. ³Department of Translational Research and New Technologies in Medicine and Surgery, University of Pisa, Pisa, Italy. ⁴The Edgar L. and Harold H. Buttner Chair of Electrical Engineering and Computer Sciences, University of California, Berkeley, CA, USA. ⁵e4life srl, Via Giorgio Vasari 4, Rome 00196, Italy. ✉email: pietro.bia@elt.it

as a promising avenue for non-chemical decontamination strategies^{19–21,23–25}. This approach shows significant promise for real-time air decontamination, primarily aimed at mitigating the spread of airborne respiratory pathogens^{23,24}. The mechanism exploits the confined acoustic dipolar mode of resonance in viral particles²⁶. When aerosolized viruses are exposed to microwave radiation at specific frequencies, energy is transferred to the virions' confined acoustic vibrational modes^{25,26}. This energy transfer induces resonance, leading to structural disruption and subsequent inactivation of the viral particles^{25,26}. Recent studies have demonstrated the effectiveness of this method against various strains of SARS-CoV-2, including the Wuhan, delta, and omicron variants^{21,23,24}. Experiments conducted in a controlled bioaerosol system revealed that exposure to microwave radiation resulted in an average reduction of 91.31% in viral titer across these variants²³. Comparable levels of inactivation were observed for the H1N1 influenza virus, achieving a 90% reduction in viral titer²⁴. However, notable differences in the optimal parameters for inactivation were identified between SARS-CoV-2 and H1N1 influenza virus²⁴. While SARS-CoV-2 showed sensitivity to frequencies up to 12 GHz, the H1N1 influenza virus exhibited susceptibility to higher frequencies, up to 16 GHz²¹. The duration of exposure also emerged as a critical factor, with SARS-CoV-2 demonstrating a ten-fold reduction in infectivity within one minute^{23,24}, while the H1N1 influenza virus required five minutes to achieve comparable levels of inactivation²⁴.

Given the ongoing global concern regarding the A(H5N1) virus and its potential impact on animal and human health^{5,6}, this study was designed to evaluate the efficacy of microwave radiation for inactivating aerosolized A(H5N1) virus particles. The investigation had two primary objectives. First, using a frequency step size approach, we sought to identify the most suitable frequency band to maximize virucidal activity against A(H5N1). Second, we examined how the microwave application time affected the inactivation elicited by microwave illumination.

Methods

Experimental setup

All tests were conducted in accordance with the established guidelines for exposure setups in biological experiments²⁷. The experimental protocol for investigating the effects of microwave radiation on aerosolized A(H5N1) virus comprised five principal stages. Initially, the virus was propagated in Madin-Darby canine kidney (MDCK) cells to generate a high-titer suspension suitable for subsequent aerosolization. This stage was crucial in ensuring a sufficient viral load for the experiments and maintaining consistency across trials. Following the preparatory phase, the viral suspension underwent a controlled aerosolization process to create a fine mist of airborne particles. This step simulated real-world conditions of A(H5N1) viral transmission and allowed for the assessment of microwave radiation effects on suspended viral particles. The aerosolized virus was then subjected to microwave exposure under rigorously controlled conditions. To elucidate the optimal parameters for viral inactivation, a systematic evaluation of various frequency bands was conducted. This approach facilitated the identification of specific frequency ranges that demonstrated maximal efficacy in viral inactivation. To further enhance our understanding of the microwave inactivation process, a temporal optimization study was performed. This experiment aimed to elucidate the relationship between exposure duration and inactivation efficacy, providing insights into the kinetics of A(H5N1) inactivation under microwave radiation.

Propagation of the A(H5N1) virus

The propagation of the A(H5N1) virus was conducted in a Biosafety Level 3 (BSL-3) laboratory at ViroStatics srl, located within the Scientific and Technological Park Porto Conte Ricerche srl (Alghero, Italy). MDCK cells, obtained from the American Type Culture Collection (Manassas, VA, USA), were maintained at 37 °C in a 5% CO₂ atmosphere. The cells were cultured in Dulbecco's Modified Eagle's Medium (DMEM) supplemented with 10% fetal bovine serum (FBS; Biowest, Nuaille, France), 1% penicillin/streptomycin antibiotic solution (Biowest), and 1% L-glutamine (Biowest). Following propagation of the live highly pathogenic avian influenza virus (H5N1) A/ck/Israel/65/10, infectious titers were quantified using the standard 50% tissue culture infectious dose (TCID₅₀) assay in MDCK cells. Upon achieving a high titer ($> 1 \times 10^5$ TCID₅₀/mL) of the A(H5N1) strain, a stock suspension was prepared for subsequent aerosolization experiments.

Aerosolization of the A(H5N1) viral suspension

All experimental procedures were carried out at a controlled temperature of 21 °C. Furthermore, the BSL-3 laboratory operator was blinded to the details of the virus inactivation protocol, ensuring that all tests were conducted under blinded conditions. The A(H5N1) viral suspension was aerosolized using a commercially available aerosol generator (Omron, Kyoto, Japan) to produce particles up to 1 µm in size within a 32 L plastic, air-proof container. This aerosolization process was designed to mimic the natural airborne transmission of the virus, simulating the droplets and aerosols that would be produced during respiratory events such as coughing, sneezing, or talking. The use of a sealed container ensured containment of the aerosolized virus for controlled exposure to the subsequent microwave treatment. The aerosolization process continued until the virus occupied the entire volume of the chamber, ensuring homogeneous distribution.

Microwave exposure

The aerosolized A(H5N1) virus was subjected to microwave radiation generated by a radio frequency (RF) generator, a custom-designed apparatus previously described in detail^{23,24}. In brief, this RF system was specifically engineered for controlled microwave radiation delivery in virus inactivation studies. The system comprised the following components: an ultra-wideband frequency-tunable synthesizer capable of operating across the C band to the Ku band, allowing for the testing of a broad range of frequencies; medium power and high-power microwave amplifiers to enhance signal strength; a digital variable attenuator to regulate

output power; and embedded software written in C++ on the ESP32 platform using Visual Studio Code, which controlled all possible configurations of the RF components. The final power amplifier of the demonstrator employed cutting-edge 0.15 μm GaN on SiC solid-state high-electron-mobility transistor technology, capable of delivering up to 10 W across an ultra-wideband range. The transmitter's RF output was connected to a horn antenna using an RF cable. This setup generated an electromagnetic field with a strength of 200 V/m in proximity to the antenna and 40 V/m at the vertices of the chamber containing the aerosolized virus. These values represent mean field amplitudes measured across the 8–16 GHz band under the antenna and averaged for all corners. These measurements were consistent with electromagnetic simulations performed at 8 GHz (Fig. 1) using CST Studio Suite (Dassault systems, Seattle, WA, USA). Based on the measured field values, the power density distribution within the chamber was determined using the Poynting vector formulation under free-space conditions (characteristic impedance $Z_0 = 377 \Omega$). The resultant power densities ranged from 4.24 W/m² at the chamber corners to 106.2 W/m² directly beneath the antenna. Notably, the whole-body exposure limit, considering the expected exposure paradigm as uncontrolled exposure in the air, is 10 W/m² averaged over 30 min, as per IEEE standards²². Based on the measured mean value of 40 V/m at the chamber corners, the corresponding power density was calculated as follows:

$$\frac{1600 \text{ W}}{377 \text{ m}^2} \times \frac{10 \text{ min}}{30 \text{ min}} = 1.4 \text{ W/m}^2 \text{ (averaged over 30min)}$$

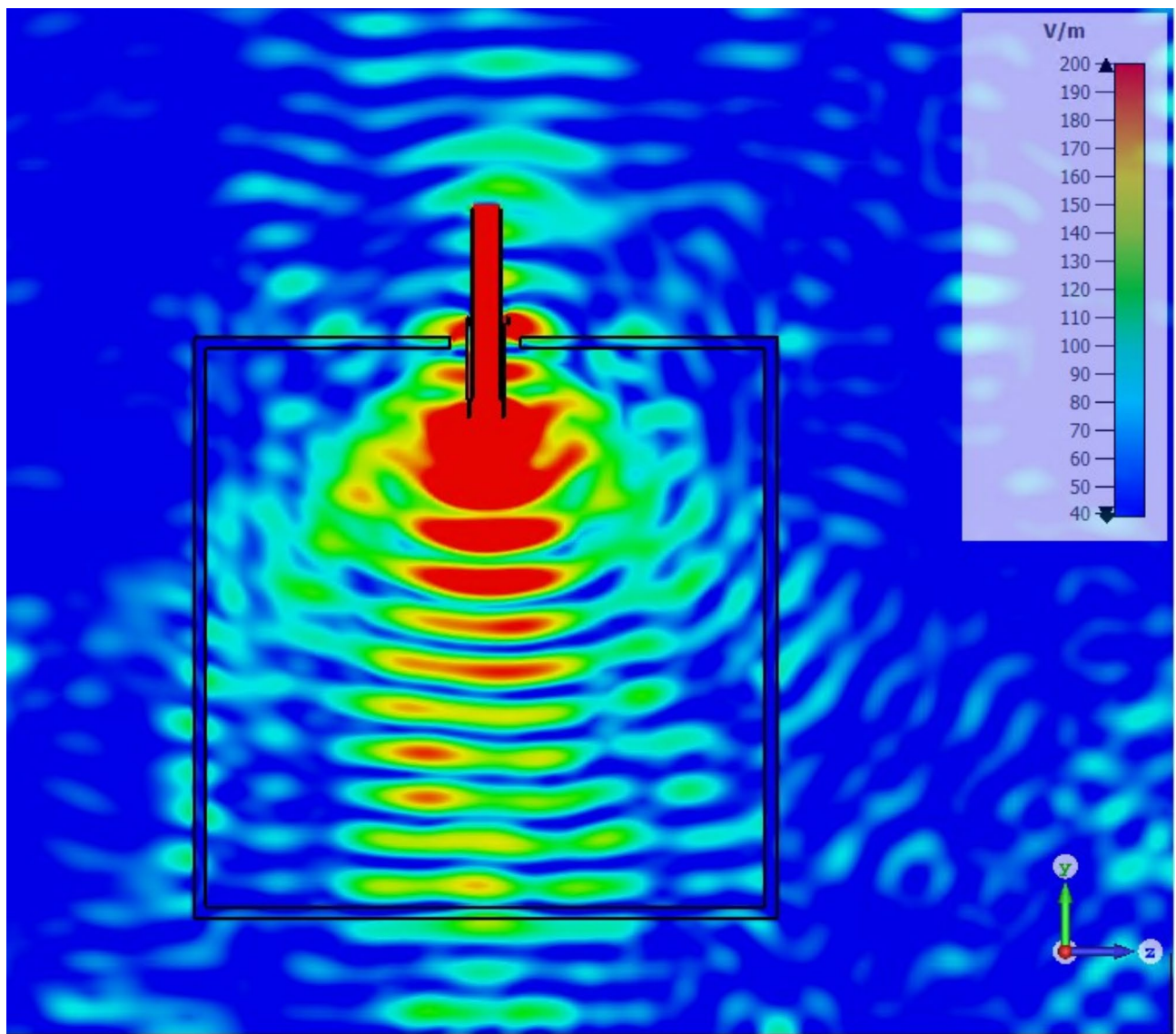


Fig. 1. Simulation of electromagnetic field intensity from an antenna operating at 8 GHz. The color map represents the electric field strength in volts per meter (V/m), with red indicating higher intensity and blue indicating lower intensity.

The resulting power density represents 14.3% of the permissible exposure level when time-averaged over a 30-min interval. For the shorter exposure durations investigated in this study (1, 3, and 5 min), the normalized power densities correspond to 1.43%, 4.29%, and 7.14% of the IEEE standard limit²², respectively. These values were derived by applying temporal scaling factors of 0.033, 0.1, and 0.167 (representing the ratio of exposure duration to the 30-min averaging period) to the reference power density. Therefore, the resultant exposure levels are substantially lower than the established thresholds known to cause thermal discomfort in humans. The designed setup enabled precise control over the frequency band and exposure time. Prior to each experiment, the system was calibrated using a broadband field meter to ensure accurate assessment of the electromagnetic field's inactivation potency at specific frequencies²³.

Optimization of the frequency band

In a series of experiments designed to optimize the frequency band for viral inactivation, aerosolized viral samples were systematically exposed to microwave radiation. Each sample was subjected to a standardized 10-minute microwave exposure period. To comprehensively assess the inactivation efficacy of microwave radiation on aerosolized A(H5N1) virus, seven distinct frequency bands were evaluated: 8–10 GHz, 9–11 GHz, 10–12 GHz, 11–13 GHz, 12–14 GHz, 13–15 GHz, and 14–16 GHz. Tests for each frequency band were performed in duplicate. Control samples consisted of aerosolized viral specimens that were not subjected to microwave illumination, with the RF source remaining inactive for the entire 10-minute exposure duration. Following the microwave treatment, the irradiated aerosol was recovered through a process of active impingement²⁰. This recovery method involved the direct collection of the treated aerosol into a glass collector containing complete medium supplemented with 2% FBS. The glass collector was equipped with an inlet and tangential nozzles, facilitating the efficient suction of air from the plastic chamber when a vacuum was applied at a rate of 12 L/min. This collection process ensured the preservation of the treated viral particles for subsequent analysis and quantification of inactivation efficacy across the various frequency bands tested. Results were expressed using two complementary methods to ensure comprehensive representation of the experimental outcomes. First, mean virus titers were calculated based on the TCID₅₀ assay, providing a quantitative measure of viral infectivity. Second, viral inactivation ratios were computed by comparing the titers of illuminated samples to those of unilluminated controls. These ratios were presented as means derived from a minimum of two independent experiments.

Optimization of the exposure time

After identifying the optimal frequency band for inactivating aerosolized A(H5N1) virus, we investigated the influence of exposure duration on inactivation efficacy. Our objective was to reduce the total exposure time from the initial 10-minute duration employed in preceding experiments, with the primary aim of identifying the minimum microwave illumination time required for effective viral inactivation. To achieve this goal, we evaluated three distinct exposure durations: 5 min, 3 min, and 1 min within the previously determined optimal frequency band. Each duration was subjected to triplicate testing. Aerosolized virus samples were subjected to microwave radiation using these parameters, and the residual viral infectivity was subsequently assessed. To quantify the results, we calculated and reported mean virus titers from the TCID₅₀ assay. Additionally, we computed viral inactivation ratios by comparing microwave-exposed samples to unilluminated controls, based on at least triplicate experiments.

Uncertainty quantification

To ensure a reliable representation of viral inactivation, an uncertainty propagation method was applied. This approach systematically incorporates the variability inherent in both control and test measurements, yielding an interval of possible inactivation values. The boundaries of this range were determined using the following equations: minimum inactivation = $\frac{(C_M - C_E) - (T_M + T_E)}{C_M - C_E}$ and maximum inactivation = $\frac{(C_M + C_E) - (T_M - T_E)}{C_M + C_E}$, where C_M represents the mean value of the control measurement, C_E denotes the absolute error associated with the control measurement, T_M signifies the mean value of the test measurement, and T_E indicates the absolute error associated with the test measurement. The resulting uncertainty in viral inactivation was expressed as a range, defined by its calculated minimum and maximum values.

Results

Efficacy of microwave radiation for inactivating aerosolized a(H5N1) virus across different frequency bands

The inactivation efficacy of microwave radiation on aerosolized A(H5N1) virus as a function of frequency band is summarized in Table 1. A non-linear frequency-dependent effect on viral inactivation was observed, with distinct patterns of efficacy across the tested frequency bands (Fig. 2). The most pronounced inactivation was achieved in the 11–13 GHz frequency band, particularly within the 11–12 GHz band, leading to a mean reduction of 89% in viral titer (range: 88–90%). This was closely followed by the 8–10 GHz band, which demonstrated a mean reduction of 83% (range: 78–88%). The 10–12 GHz band also exhibited significant inactivation, with a mean reduction of 79% (range: 76–83%). Notably, the 9–11 GHz band displayed a somewhat lower, yet still substantial, inactivation efficacy with a mean reduction of 66% (range: 61–70%). In contrast, the higher frequency bands demonstrated a lack of inactivation efficacy. Specifically, the 12–14 GHz, 13–15 GHz, and 14–16 GHz ranges showed minimal to no reduction in viral titer compared to the unirradiated control. The mean viral titers for these frequency bands were comparable to or even slightly higher than the control, although this

Frequency band, GHz	Mean viral titer, TCID ₅₀ /mL	Mean percentage reduction compared to control
Unirradiated control	26,300	–
8–10	4390	83
9–11	8970	66
10–12	5480	79
11–13	2870	89
12–14	26,800	0
13–15	25,700	2
14–16	29,400	0

Table 1. Effect of microwave frequency bands on a(H5N1) viral titer reduction. Percentage reduction was calculated relative to the unirradiated control, showing mean values observed across replicates. Abbreviation: TCID₅₀, 50% tissue culture infective dose.

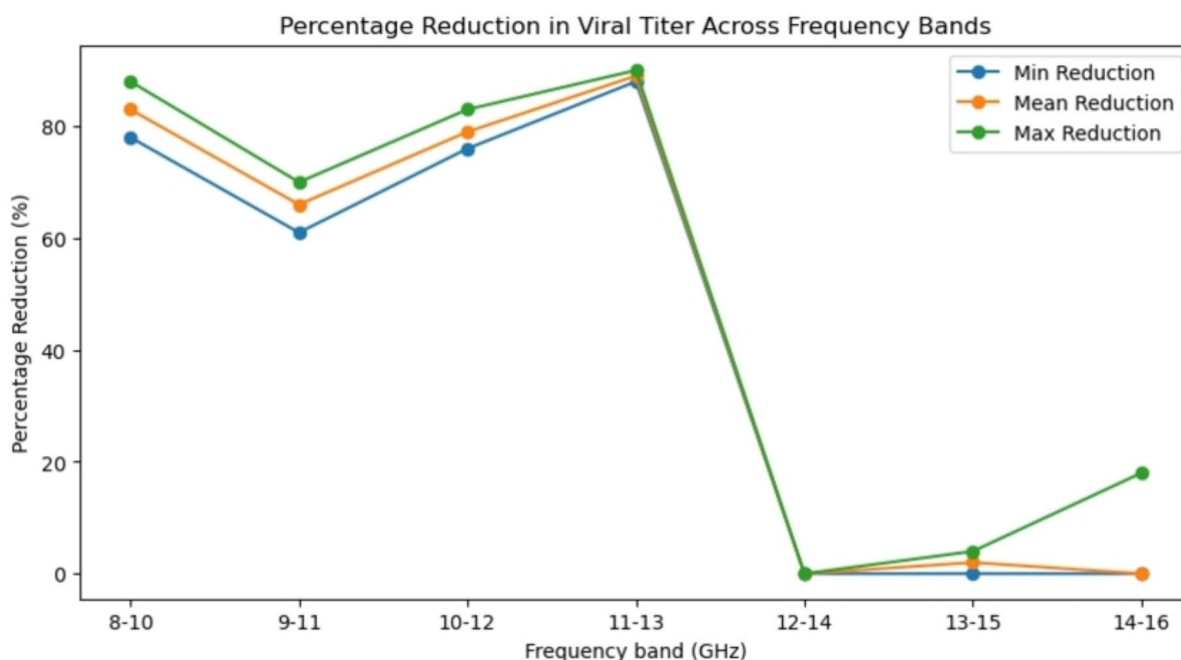


Fig. 2. Percentage reduction in A(H5N1) viral titers across different microwave frequency bands.

difference is likely within the margin of experimental error. Based on these findings and the previous success in achieving approximately 90% inactivation of SARS-CoV-2^{23,24}, a frequency band of 8–12 GHz was selected for further evaluation in optimizing exposure time experiments. This choice was motivated by the observed efficacy within this frequency range and its potential to effectively inactivate both A(H5N1) and SARS-CoV-2 viruses, suggesting a broader applicability of this approach across different viral pathogens.

Time-dependent efficacy of microwave radiation for inactivating aerosolized a(H5N1) virus

Following the optimization of the frequency band, we investigated the impact of exposure duration on the efficacy of microwave radiation for inactivating aerosolized A(H5N1) virus. The results, summarized in Table 2, demonstrate a clear time-dependent effect on viral inactivation within the 8–12 GHz frequency band. A positive correlation between exposure time and viral inactivation efficacy was observed (Fig. 3). Notably, the 5-minute exposure period demonstrated optimal efficacy, yielding a mean viral titer reduction of 94% (range: 92–95%). The narrow range of outcomes indicates high consistency, suggesting that this duration was sufficient to achieve robust and reproducible viral inactivation. In contrast, a 3-minute exposure resulted in moderate inactivation, with a mean reduction of 58% (range: 29–74%). The broader range observed in this condition suggests greater variability in outcomes, potentially due to the exposure time approaching a critical threshold for effective inactivation. Notably, a brief 1-minute exposure yielded a mean reduction of 48% (range: 0–76%). The substantial variability in results, ranging from no effect to significant inactivation, indicates that this duration is insufficient to ensure consistent virucidal activity.

Exposure time, min	Mean viral titer, TCID ₅₀ /mL	Mean percentage reduction compared to control
Unirradiated control	1670	–
5	100	94
3	698	58
1	861	48

Table 2. Effect of microwave irradiation time on a(H5N1) viral titer reduction. Percentage reduction is calculated relative to the unirradiated control, showing mean values observed across replicates. Abbreviation: TCID₅₀, 50% tissue culture infective dose.

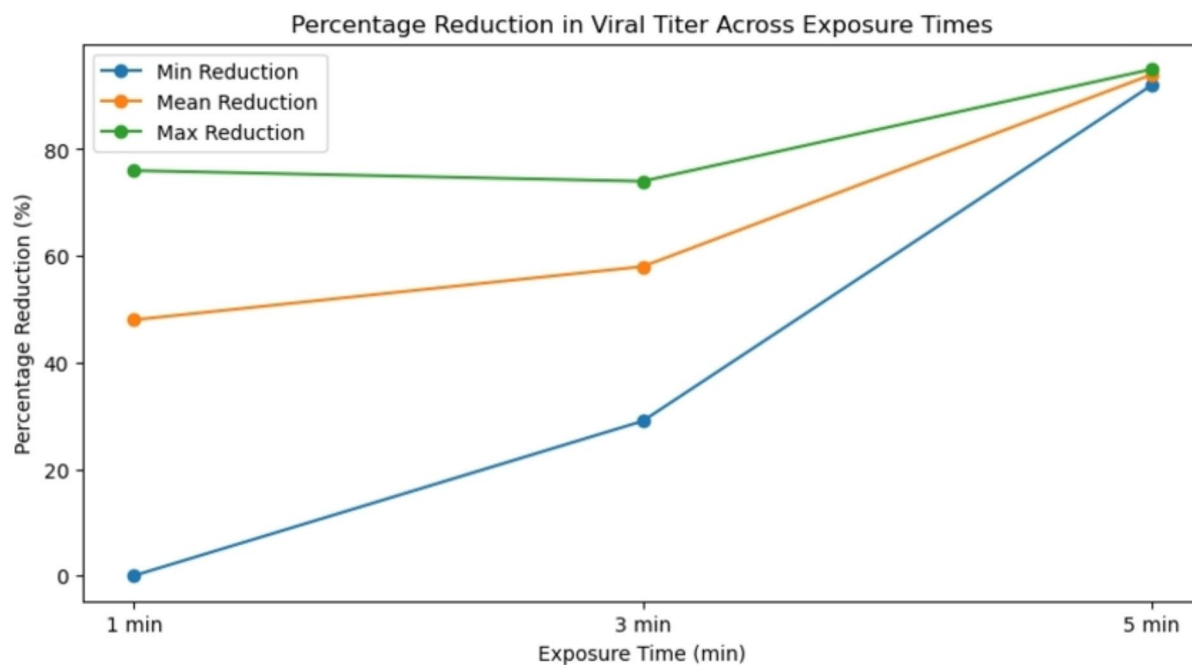


Fig. 3. Percentage reduction in A(H5N1) viral titers across different exposure times.

Discussion

Recent epidemics and pandemics of respiratory viruses – including the 2003 severe acute respiratory syndrome outbreak, the 2009 H1N1 influenza pandemic, the 2012 Middle East respiratory syndrome coronavirus outbreak, and the COVID-19 pandemic caused by SARS-CoV-2²⁸ – have necessitated a critical reassessment of existing strategies for viral containment and prevention. Notably, a recent Cochrane review suggested that relying exclusively on antiviral medications and vaccines may be insufficient to effectively interrupt or mitigate the spread of acute respiratory viruses²⁹. In response to these challenges, microwave inactivation of airborne microorganisms has emerged as a promising non-chemical technology for viral inactivation^{17,19–21,23–25}.

This is, to our knowledge, the first study to examine the inactivation efficacy of microwave illumination against aerosolized avian influenza A(H5N1) virus. Our research, aimed at optimizing the approach to maximize virucidal activity against an airborne pathogen currently under close surveillance^{5,6,10}, yielded two principal findings. First, our analysis revealed that the optimal frequency range for inactivating A(H5N1) in an aerosolized state lies between 11 and 13 GHz, resulting in a substantial mean reduction of 89% in viral titer. Second, we unequivocally demonstrated the time-dependent nature of A(H5N1) viral inactivation, revealing a positive correlation between exposure duration and inactivation efficacy.

With respect to viral inactivation in response to the frequency range generated by the RF-wave emission system, A(H5N1) exhibited susceptibility up to 13 GHz. This threshold is lower than our previously observed value for the H1N1 human influenza virus (up to 16 GHz)²⁴ but aligns with the sensitivity of SARS-CoV-2 (up to 12 GHz)²³. Consequently, for subsequent experiments aimed at verifying the effect of exposure time on viral inactivation, we selected an 8–12 GHz frequency band to encompass both A(H5N1) and SARS-CoV-2 susceptibility ranges. Importantly, the similar optimal frequency ranges observed for diverse viruses hint at a common biophysical basis for microwave susceptibility among enveloped viruses. This could potentially allow for the development of generalized microwave-based disinfection protocols effective against a wide range of viral threats^{25,26}. In this regard, the effectiveness of the 8–12 GHz frequency band may be attributed to its resonance with the confined acoustic vibrational modes of viral particles, as proposed by the structure resonance energy transfer (SRET)

model²⁶. This resonance effect likely induces structural disruptions in viral components, ultimately leading to loss of infectivity. The SRET mechanism, as described by Yang et al.²⁶, suggests that microwaves of the same frequency can resonantly excite the dipolar mode of the confined acoustic vibrations inside virions. This process, known as microwave resonant absorption, is influenced by various factors including the virus's hydration level, surface charge, size, and surrounding media²⁶. Our current findings on the inactivation of aerosolized A(H5N1) virus align with previous studies demonstrating the virucidal effects of non-thermal microwaves against various virions in different media – including SARS-CoV-2 and H1N1 influenza virus in aerosol form^{23,24}, SARS-CoV-2 in deionized water³⁰, H3N2 influenza virus²⁵ and bovine coronavirus (BCoV)³¹ in aqueous solutions, human coronavirus HCoV-229E in culture medium³², and the BCoV on dry surfaces³³. The time-dependent nature of A(H5N1) inactivation observed in our study corroborates previous observations showing time-dependent inactivation of both SARS-CoV-2 and H1N1 in aerosols using microwave illumination^{23,24}. Accordingly, our current results demonstrate that longer exposure times lead to more consistent and effective viral inactivation, with the 5-minute exposure striking an optimal balance between high efficacy and practical application time.

Several methodological limitations warrant careful consideration in interpreting the present findings. While our experimental setup was intentionally designed to closely simulate real-world conditions, we recognize that variables such as ambient humidity, temperature fluctuations, and the presence of organic matter may substantially influence inactivation efficacy. Importantly, the methodology employed in the present study differs from that of Banting et al.³², who developed a system specifically optimized for precise control over electromagnetic field distribution using custom-designed microwave guide sections. However, their approach represents a significant departure from the dynamic and variable conditions typically encountered in fluid dynamics under real-world scenarios. In contrast, our study prioritized ecological validity by employing a setup that more accurately reflects realistic environmental conditions, despite the inherent challenges posed by variability in electric field intensity across temporal, spatial, and frequency domains. Our research demonstrates the successful inactivation of aerosolized viruses; however, further studies are needed to comprehensively evaluate this approach's effectiveness against viruses in other matrices, such as surfaces and liquid media. We also acknowledge that, despite its overall effectiveness, our experimental framework has inherent limitations in quantifying process variability at intermediate stages. The system's complexity, coupled with the lack of measurable data during the aerosolization and collection phases, hindered a quantitative analysis of these potential fluctuations. As a result, our analytical scope was necessarily restricted to the downstream harvest titration stage. In addition, non-uniform field distribution within the test box and unquantified dosimetric uncertainties posed further technical challenges that warrant attention in future investigations to enhance methodological precision and experimental reproducibility. Nevertheless, it is important to emphasize that the SRET methodology primarily relies on field amplitude and is not directly dependent on dosimetric evaluations. Finally, it should be noted that no positive controls were included in this study to quantify variance or confirm expected responses. To facilitate the advancement and validation of non-thermal microwave technology for viral inactivation, future studies should systematically address these methodological caveats. Given the ongoing challenges posed by emerging and re-emerging avian influenza threats^{3,5,10}, the investigation of non-thermal microwaves in real-world environments represents a crucial next step. For instance, the implementation of microwave emitters optimized against A(H5N1) could potentially provide continuous disinfection of circulating air in high-risk environments such as poultry farms, processing facilities, and veterinary clinics. This approach could significantly mitigate the risk of airborne transmission in these settings.

Conclusions

This study demonstrates the efficacy of microwave radiation in inactivating aerosolized A(H5N1) virus. Notably, our results revealed a clear time-dependent effect on viral inactivation within the 8–12 GHz frequency band, with a 5-minute exposure demonstrating optimal efficacy. This exposure duration yielded the most consistent and effective viral inactivation, resulting in a mean viral titer reduction of 94% (range: 92–95%). These findings corroborate previous research on other enveloped viruses, indicating a shared biophysical foundation for microwave susceptibility. This commonality could pave the way for the development of broadly applicable disinfection protocols. While further research is needed to address limitations and explore real-world applications, this non-thermal microwave approach shows promise as a novel strategy for mitigating the spread of airborne viral pathogens, including the highly pathogenic A(H5N1) influenza virus.

Data availability

Access to the datasets generated and analyzed during this study can be provided by the corresponding author upon reasonable request.

Received: 17 August 2024; Accepted: 2 January 2025

Published online: 15 January 2025

References

1. Charostad, J. et al. A comprehensive review of highly pathogenic avian influenza (HPAI) H5N1: an imminent threat at doorstep. *Travel Med. Infect. Dis.* **55**, 102638. <https://doi.org/10.1016/j.tmaid.2023.102638> (2023).
2. Szablewski, C. M. et al. Reported global avian influenza detections among humans and animals during 2013–2022: comprehensive review and analysis of available surveillance data. *JMIR Public. Health Surveill.* **9**, e46383. <https://doi.org/10.2196/46383> (2023).
3. Xie, R. et al. The episodic resurgence of highly pathogenic avian influenza H5 virus. *Nature* **622**, 810–817. <https://doi.org/10.1038/s41586-023-06631-2> (2023).

4. Pulit-Penaloza, J. A. et al. Highly pathogenic avian influenza A(H5N1) virus of clade 2.3.4.4b isolated from a human case in Chile causes fatal disease and transmits between co-housed ferrets. *Emerg. Microbes Infect.* **13**, 2332667. <https://doi.org/10.1080/22221751.2024.2332667> (2024).
5. Al-Tawfiq, J. A., Tirupathi, R. & Tamsah, M. H. Feathered fears: could avian H5N1 influenza be the next pandemic threat of disease X? *New. Microbes New. Infect.* **59**, 101416. <https://doi.org/10.1016/j.nmni.2024.101416> (2024).
6. Zhang, Z. & Lei, Z. The alarming situation of highly pathogenic avian influenza viruses in 2019–2023. *Glob Med. Genet.* **11**, 200–213. <https://doi.org/10.1055/s-0044-1788039> (2024).
7. Wong, S. S. & Yuen, K. Y. Avian influenza virus infections in humans. *Chest* **129**, 156–168. <https://doi.org/10.1378/chest.129.1.156> (2006).
8. Uyeki, T. M. & Bresee, J. S. Detecting human-to-human transmission of avian influenza A (H5N1). *Emerg. Infect. Dis.* **13**, 1969–1971. <https://doi.org/10.3201/eid1312.071153> (2007).
9. Kang, M. et al. Zoonotic infections by avian influenza virus: changing global epidemiology, investigation, and control. *Lancet Infect. Dis.* **24**, e522–e531. [https://doi.org/10.1016/S1473-3099\(24\)00234-2](https://doi.org/10.1016/S1473-3099(24)00234-2) (2024).
10. Kojima, N. et al. Building global preparedness for avian influenza. *Lancet* **403**, 2461–2465. [https://doi.org/10.1016/S0140-6736\(24\)00934-6](https://doi.org/10.1016/S0140-6736(24)00934-6) (2024).
11. Sun, W. et al. Natural reassortment of eurasian avian-like swine H1N1 and avian H9N2 influenza viruses in pigs, China. *Emerg. Infect. Dis.* **28**, 1509–1512. <https://doi.org/10.3201/eid2807.220642> (2022).
12. Adlhoch, C. & Baldinelli, F. Avian influenza, new aspects of an old threat. *Euro. Surveill.* **28**, 2300227. <https://doi.org/10.2807/1560-7917.ES.2023.28.19.2300227> (2023).
13. Kanaujia, R. et al. Avian influenza revisited: concerns and constraints. *Virusdisease* **33**, 456–465. <https://doi.org/10.1007/s13337-022-00800-z> (2022).
14. van Riel, D. et al. Human and avian influenza viruses target different cells in the lower respiratory tract of humans and other mammals. *Am. J. Pathol.* **171**, 1215–1223. <https://doi.org/10.2353/ajpath.2007.070248> (2007).
15. Chan, M. C. et al. Proinflammatory cytokine responses induced by influenza A (H5N1) viruses in primary human alveolar and bronchial epithelial cells. *Respir Res.* **6**, 135. <https://doi.org/10.1186/1465-9921-6-135> (2005).
16. Gruber, P. C., Gomersall, C. D. & Joynt, G. M. Avian influenza (H5N1): implications for intensive care. *Intensive Care Med.* **32**, 823–829. <https://doi.org/10.1007/s00134-006-0148-z> (2006).
17. Xiao, Y., Zhao, L. & Peng, R. Effects of electromagnetic waves on pathogenic viruses and relevant mechanisms: a review. *Virol. J.* **19**, 161. <https://doi.org/10.1186/s12985-022-01889-w> (2022).
18. Hoff, B. W. et al. Observed reductions in the infectivity of bioaerosols containing bovine coronavirus under repetitively pulsed RF exposure. *IEEE Trans. Biomed. Eng.* **70**, 640–649. <https://doi.org/10.1109/TBME.2022.3199333> (2023).
19. Wu, Y. & Yao, M. In situ airborne virus inactivation by microwave irradiation. *Chin. Sci. Bull.* **59**, 1438–1445. <https://doi.org/10.1007/s11434-014-0171-3> (2014).
20. Wang, C., Hu, X. & Zhang, Z. Airborne disinfection using microwave-based technology: energy efficient and distinct inactivation mechanism compared with waterborne disinfection. *J. Aerosol Sci.* **137**, 105437. <https://doi.org/10.1016/j.jaerosci.2019.105437> (2019).
21. Wang, P. J. et al. Microwave resonant absorption of SARS-CoV-2 viruses. *Sci. Rep.* **12**, 12596. <https://doi.org/10.1038/s41598-022-16845-5> (2022).
22. Bailey, W. H. et al. Synopsis of IEEE Std C95.1™–2019 IEEE standard for safety levels with respect to human exposure to electric, magnetic, and electromagnetic fields, 0 hz to 300 GHz. *IEEE Access.* **7**, 171346–171356. <https://doi.org/10.1109/ACCESS.2019.2954823> (2019).
23. Manna, A. et al. SARS-CoV-2 inactivation in aerosol by means of radiated microwaves. *Viruses* **15**, 1443. <https://doi.org/10.3390/v15071443> (2023).
24. Manna, A. et al. Endemic respiratory viruses inactivation in aerosol by means of radiated microwaves. *Med. Res. Arch.* **11**, 11. <https://doi.org/10.18103/mra.v11i10.4486> (2023).
25. Sadraei, M., Kabakova, I., Zhou, J. & Jin, D. Virus inactivation by matching the vibrational resonance. *Appl. Phys. Rev.* **11**, 021324. <https://doi.org/10.1063/5.0183276> (2024).
26. Yang, S. C. et al. Efficient structure resonance energy transfer from microwaves to confined acoustic vibrations in viruses. *Sci. Rep.* **5**, 18030. <https://doi.org/10.1038/srep18030> (2015).
27. Kuster, N. & Schönborn, F. Recommended minimal requirements and development guidelines for exposure setups of bio-experiments addressing the health risk concern of wireless communications. *Bioelectromagnetics* **21**, 508–514. [https://doi.org/10.1002/1521-186x\(200010\)21:7%3C508::aid-bem4%3E3.0.co;2-f](https://doi.org/10.1002/1521-186x(200010)21:7%3C508::aid-bem4%3E3.0.co;2-f) (2000).
28. Baker, R. E. et al. Infectious disease in an era of global change. *Nat. Rev. Microbiol.* **20**, 193–205. <https://doi.org/10.1038/s41579-021-00639-z> (2022).
29. Jefferson, T. et al. Physical interventions to interrupt or reduce the spread of respiratory viruses. *Cochrane Database Syst. Rev.* **1**, CD006207. <https://doi.org/10.1002/14651858.CD006207.pub6> (2023).
30. Afaghi, P., Lapolla, M. A. & Ghandi, K. Denaturation of the SARS-CoV-2 spike protein under non-thermal microwave radiation. *Sci. Rep.* **11**, 23373. <https://doi.org/10.1038/s41598-021-02753-7> (2021).
31. Cantu, J. C. et al. Evaluation of inactivation of bovine coronavirus by low-level radiofrequency irradiation. *Sci. Rep.* **13**, 9800. <https://doi.org/10.1038/s41598-023-36887-7> (2023).
32. Banting, H. et al. Electromagnetic deactivation spectroscopy of human coronavirus 229E. *Sci. Rep.* **13**, 8886. <https://doi.org/10.1038/s41598-023-36030-6> (2023).
33. Echchgadda, I. et al. Evaluation of viral inactivation on dry surface by high peak power microwave (HPPM) exposure. *Bioelectromagnetics* **44**, 5–16. <https://doi.org/10.1002/bem.22435> (2023).

Acknowledgements

This project was sponsored by an unrestricted grant from Elettronica S.p.A. (Rome, Italy).

Author contributions

Conceptualization: P.B., A.M., S.B., G.P.P.; Methodology: P.B., A.M., S.B., G.P.P., A.S.V.; Experiment: P.B., M.L., A.M.; Analysis: P.B., M.L., A.M.; Device Fabrication: P.B., M.L., A.M.; Funding acquisition: A.M.; Supervision: S.B., G.P.P., A.S.V.; Writing – drafting: P.B., M.L., A.M.; Writing – review: S.B., G.P.P., A.S.V.

Declarations

Competing interests

A.M., P.B. and M.L. are employees of Elettronica S.p.A. The remaining authors declare that they have no conflicts of interest related to this work.

Additional information

Correspondence and requests for materials should be addressed to P.B.

Reprints and permissions information is available at www.nature.com/reprints.

Publisher's note Springer Nature remains neutral with regard to jurisdictional claims in published maps and institutional affiliations.

Open Access This article is licensed under a Creative Commons Attribution-NonCommercial-NoDerivatives 4.0 International License, which permits any non-commercial use, sharing, distribution and reproduction in any medium or format, as long as you give appropriate credit to the original author(s) and the source, provide a link to the Creative Commons licence, and indicate if you modified the licensed material. You do not have permission under this licence to share adapted material derived from this article or parts of it. The images or other third party material in this article are included in the article's Creative Commons licence, unless indicated otherwise in a credit line to the material. If material is not included in the article's Creative Commons licence and your intended use is not permitted by statutory regulation or exceeds the permitted use, you will need to obtain permission directly from the copyright holder. To view a copy of this licence, visit <http://creativecommons.org/licenses/by-nc-nd/4.0/>.

© The Author(s) 2025